JVI Journals.ASM.org

Quantitative Proteomics Identifies Host Factors Modulated during Acute Hepatitis E Virus Infection in the Swine Model

Sophie Rogée,[a,b,c] Morgane Le Gall,[d,e,f] Philippe Chafey,[d,e,f] Jérôme Bouquet,[a,b,c] Nathalie Cordonnier,[a,b,c] Christian Frederici,[d,e,f] Nicole Pavio[a,b,c]

UMR 1161 Virology, ANSES, Laboratoire de Santé Animale, Maisons-Alfort, France[a]; UMR 1161 Virology, INRA, Maisons-Alfort, France[b]; UMR 1161 Virology, Ecole Nationale Vétérinaire d'Alfort, Maisons-Alfort, France[c]; INSERM, U1016, Institut Cochin, Plateforme de Proteomique, Paris, France[d]; Université Paris Descartes, Sorbonne Paris Cité, Paris, France[e]; CNRS, UMR8104, Paris, France[f]

ABSTRACT

Hepatitis E virus (HEV) causes acute enterically transmitted hepatitis. In industrialized countries, it is a zoonotic disease, with swine being the major reservoir of human HEV contamination. The occurrence and severity of the disease are variable, with clinical symptoms ranging from asymptomatic to self-limiting acute hepatitis, chronic infection, or fulminant hepatitis. In the absence of a robust cell culture system or small-animal models, the HEV life cycle and pathological process remain unclear. To characterize HEV pathogenesis and virulence mechanisms, a quantitative proteomic analysis was carried out to identify cellular factors and pathways modulated during acute infection of swine. Three groups of pigs were inoculated with three different strains of swine HEV to evaluate the possible role of viral determinants in pathogenesis. Liver samples were analyzed by a differential proteomic approach, two-dimensional difference in gel electrophoresis, and 61 modulated proteins were identified by mass spectroscopy. The results obtained show that the three HEV strains replicate similarly in swine and that they modulate several cellular pathways, suggesting that HEV impairs several cellular processes, which can account for the various types of disease expression. Several proteins, such as heterogeneous nuclear ribonucleoprotein K, apolipoprotein E, and prohibitin, known to be involved in other viral life cycles, were upregulated in HEV-infected livers. Some differences were observed between the three strains, suggesting that HEV's genetic variability may induce variations in pathogenesis. This comparative analysis of the liver proteome modulated during infection with three different strains of HEV genotype 3 provides an important basis for further investigations on the factors involved in HEV replication and the mechanism of HEV pathogenesis.

IMPORTANCE

Hepatitis E virus (HEV) is responsible for acute hepatitis, with clinical symptoms ranging from asymptomatic to self-limiting acute hepatitis, chronic infection, or fulminant hepatitis. In industrialized countries, HEV is considered an emerging zoonotic disease, with swine being the principal reservoir for human contamination. The viral and cellular factors involved in the replication and/or pathogenesis of HEV are still not fully known. Here we report that several cellular pathways involved in cholesterol and lipid metabolism or cell survival were modulated during HEV infection in the swine model. Moreover, we observed a difference between the different swine strains, suggesting that HEV's genetic variability could play a role in pathogenesis. We also identified some proteins known to be involved in other viral cycles. Our study provides insight into the mechanisms modulated during HEV infection and constitutes a useful reference for future work on HEV pathogenesis and virulence.

Hepatitis E virus (HEV) is responsible for major epidemics of acute hepatitis in low- and middle-income countries worldwide. In industrialized countries, it is an emerging problem, as an increasing number of sporadic cases have been reported in patients who have never traveled to areas where HEV is endemic. The evolution of hepatitis E is often benign, but severe forms or chronic infections have been described. A high rate of fulminant hepatitis has been reported in pregnant women (20%) (1, 2) and patients suffering from other liver diseases, such as hepatitis C virus (HCV) or hepatitis B virus (HBV) coinfection (3, 4). Chronic HEV infections occur in immunosuppressed patients, such as solid-organ transplant recipients (5). More recently, several neurological symptoms, such as Guillain-Barré or Parsonage-Turner syndrome, were linked to HEV infections. The mechanisms responsible for the different degrees of hepatitis E severity are not clearly understood, though both host and viral factors are probably involved.

HEV is a nonenveloped, single-stranded, positive-sense RNA virus classified in the *Hepeviridae* family (6). The genome is 7.2 kb in length and contains three major open reading frames (ORFs). ORF1 encodes a nonstructural protein with several functional motifs, methyltransferase, papain-like cysteine protease, RNA helicase, and RNA-dependent RNA polymerase (7–10). ORF2 and ORF3 overlap, and the two proteins are translated from a single

Received 29 July 2014 **Accepted** 2 October 2014

Accepted manuscript posted online 15 October 2014

Citation Rogée S, Le Gall M, Chafey P, Bouquet J, Cordonnier N, Frederici C, Pavio N. 2015. Quantitative proteomics identifies host factors modulated during acute hepatitis E virus infection in the swine model. J Virol 89:129–143. doi:10.1128/JVI.02208-14.

Editor: J.-H. J. Ou

Address correspondence to Nicole Pavio, npavio@vet-alfort.fr.

Supplemental material for this article may be found at http://dx.doi.org/10.1128/JVI.02208-14.

doi:10.1128/JVI.02208-14

subgenomic RNA (11). ORF2 encodes the unique viral capsid protein. ORF3 encodes a small phosphorylated protein of 113 to 123 amino acids, the function(s) of which has not yet been fully defined (12). The HEV replication mechanism is still not fully understood, since there is no robust model for propagating HEV *in vitro*. Furthermore, the cellular factors involved in the replication and/or virulence of HEV are still unknown.

In the recently proposed classification of HEVs, HEVs that can infect humans belong to the *Orthohepevirus* genus, *Orthohepevirus A* species, and are divided into four genotypes (HEV genotype 1 [HEV-1] to HEV-4) (13): HEV-1 and HEV-2 have been reported in humans from Asia and Africa and from Mexico and Africa, respectively. HEV-3 and HEV-4 have been identified in both human and animal species—mostly swine—in North and South America, Europe, and Asia (14). Within each genotype, several clusters can be delineated, but a classification into subtypes proposed in the literature is not recognized by the International Committee on Taxonomy of Viruses (15). These clusters are based on phylogenetic analysis, but there is no indication of the associated virulence. In some countries, there are more of certain clusters than others, but it is not known if this is due to virulence factors or ecological factors (16–18).

In countries where major epidemics are reported, the main transmission vector for hepatitis E virus infections is contaminated water or soiled food. In contrast, in countries where sporadic cases or grouped cases occur, contamination pathways are still under investigation. Confirmed zoonotic transmissions through the ingestion of raw or undercooked contaminated deer and boar meat have been described in Japan (19, 20). Several cases were also associated with the consumption of pork products containing raw liver (21).

Viral infections usually alter host cell functions, thus determining the fate of infected cells and the progression of pathogenesis. The development of proteomic methods enables changes in cellular protein expression to be investigated at a global scale and close virus-host interactions to be identified. This approach has been used to study infections caused by several viruses, including influenza virus, respiratory syncytial virus (RSV), severe acute respiratory syndrome coronavirus (SARS-CoV), human immunodeficiency virus type 1 (HIV-1), and mouse hepatitis virus (MHV) (22–25). A recent proteomic analysis of livers infected by swine hepatitis E virus identified 10 proteins that may be involved in HEV infection, especially with a modulation of apolipoprotein E (ApoE) and ferritin heavy-chain expression (26).

In the present study, global changes in the proteome profiles of pig livers infected with three different strains of swine HEV genotype 3 were investigated using two-dimensional (2D) fluorescence difference in gel electrophoresis (DIGE). To evaluate the influence of the genetic variability of HEV on pathogenesis, the three strains studied belonged to three different phylogenetic clusters (less than 90% identity in their nucleotide sequences). A total of 61 differentially expressed proteins were identified between infected and uninfected livers. Four proteins known to play a role in other viral replication cycles were upregulated in the HEV-infected liver. The overexpression of some proteins was confirmed by quantitative immunoblotting and transcript quantification by quantitative reverse transcription (RT)-PCR (qRT-PCR). Some differences were observed between the three strains studied, but overall, the proteins most affected were those involved in general metabolism, lipid and cholesterol homeostasis, trafficking, and inflammatory and immune responses. Several networks possibly involved in pathogenesis were identified.

The present study is the first to compare the biological effects of three different strains of swine HEV genotype 3 strains using a quantitative proteomic approach in a swine experimental model. The results achieved will help determine the major cellular pathways modulated during HEV infection and will support further studies on HEV pathogenesis in various contexts.

MATERIALS AND METHODS

Virus. Fecal samples from naturally or experimentally infected pigs were used as a source of swine HEV genotype 3. Viruses were previously fully sequenced and belonged to three different phylogenetic clusters with 85 to 89% identity in their nucleotide sequences: strain A (GenBank accession number JQ953664), strain B (GenBank accession number JQ953665), and strain C (GenBank accession number JQ953666). According to the classification by Lu et al. (15), strains A, B, and C clustered within subtypes 3c, 3e, and 3f, respectively. Fecal suspensions were prepared (2 g in 10% [wt/vol] phosphate buffer) and centrifuged at 4,000 × *g* and 4°C for 20 min. The resulting clear supernatant was purified by two successive passages through a microfilter with a pore size of 0.45 and then a microfilter with a pore size of 0.22 μm (Millex-GV; Millipore SAS, Molsheim, France). Aliquots of the suspensions were stored at −80°C until use.

Experimental infection. Twelve 8-week-old specifc-pathogen-free (SPF) piglets negative for anti-HEV antibodies and HEV RNA were divided into four groups of three. The first group was mock infected and inoculated intravenously with phosphate-buffered saline (PBS). The other groups were inoculated intravenously with a suspension of HEV strain A, B, or C containing 10^6 copies of HEV RNA. Their feces were collected at 3, 7, and 8 days postinoculation (p.i.). Animals were euthanized at 8 days p.i. Liver, bile, and feces were collected, and livers were immediately frozen in liquid nitrogen for proteomic analysis.

Ethics statement. This experimental protocol was validated by the ethics committee (ComEth number 12-043) of the National Veterinary School of Alfort, the French Agency for Food, Environmental and Occupational Health & Safety, and University Paris 12.

The present experimental protocol has obtained formal approval (notice number 09/10/12-9) from the ethics committee, which evaluated that (i) animals had to be used for the project, (ii) the chosen species was relevant to the scientific question, (iii) the number of animals used had been carefully adjusted, (iv) the procedures on animals were appropriate and performed by competent persons, (v) pain, stress, and discomfort had been anticipated and were minimized, and (vi) humane endpoints had been considered and planned whenever appropriate. All experiments on live animals were carried out in the Biomedical Research Center (CRBM; certification number 94-046-2) under the responsibility of Thomas Lilin, who has been certified for research activities involving live vertebrate animals (94-363, 24 October 2011), in compliance with French and European regulations on the care and protection of laboratory animals.

Histopathologic evaluation. Samples of pig liver were collected and fixed in 10% neutral buffered formalin. Tissues were then dehydrated and embedded in paraffin. Five-micrometer sections were stained with hematoxylin-eosin-saffron and observed through a Leica DM2000 microscope to evaluate histopathologic lesions.

Serum liver chemistry profile. The activities of alanine transaminase (ALT) and aspartate transaminase (AST) and the levels of cholesterol and triglyceride in sera were measured with an automated biochemistry analyzer (Olympus 2700; Olympus, Japan).

Sample preparation. Sterile surgical blades were used to excise 30 mg of liver. Tissues were incubated on ice with a lysis buffer (7 M urea, 2 M thiourea, 4% CHAPS {3-[(3-cholamidopropyl)-dimethylammonio]-1-propanesulfonate}, 2% immobilized pH gradient (IPG) buffer, 40 mM dithiothreitol, and 1% protease inhibitor mix [Roche]), disrupted in bead-milling tubes (FastPrep 24; MP Biomedicals, Illkrish, France), and

then incubated for 1 h at 4°C, centrifuged at 15,000 × *g* for 15 min at 4°C, and stored at −80°C.

2D-DIGE analysis. Twelve liver extracts (four groups and three independent biological repeats) were analyzed by 2D-DIGE as described previously (27). Briefly, each protein sample (50 μg) was labeled with CyDyes Fluor minimal dyes (GE Healthcare) according to the manufacturer's instructions. Two samples from each experimental group (namely, samples 1 and 3 from the mock-infected [group T] group and the three groups infected with strains A, B, and C [groups A to C]) were labeled with Cy3 and two samples from each experimental group were labeled with Cy5 (CyDyes DIGE Fluor minimal dyes; GE Healthcare). Equal amounts of all samples were pooled, Cy2 labeled, and used as the internal standard. Six analytical gels, each containing one sample labeled with Cy3, one sample from another group labeled with Cy5, and the internal standard labeled with Cy2, were run. Labeled samples were mixed and then loaded onto 18-cm IPG strips, pH 4 to 7 (GE Healthcare). Isoelectric focusing was performed using an IPGphor apparatus (GE Healthcare) for a total of 60 kV · h. Equilibrated strips were then placed onto homemade SDS-polyacrylamide gels (8 to 18%), and electrophoresis was performed in an Ettan-DALT II system (GE Healthcare) at 2.5 W/gel and 12°C. Gels were scanned using a Typhoon 9400 molecular imager (GE Healthcare) with the resolution set at 100 μm. Image analysis, relative quantification, statistical data analysis, and principal component analysis (PCA) were performed using Decyder 2D software (version 7.0; GE Healthcare). The fold change and Student's *t* test *P* values were calculated across pairwise comparisons (group A versus group T, group A versus group B, group A versus group C). A spot was considered differentially expressed if the fold change was larger than +1.5 or smaller than −1.5 and Student's *t* test *P* value was less than 0.05. PCA was performed on the global distribution of proteins to reveal differences under the current experimental conditions. Spots of interest were identified by mass spectrometry (MS).

Identification of protein spots by MS. For MS and MS/MS analysis on a linear trap quadrupole (LTQ)-Orbitrap mass spectrometer, two semipreparative 2D gels were prepared as described previously (28). Analyses were performed using an Ultimate 3000 rapid separation liquid chromatographic (RSLC) system (Thermo Fisher Scientific) online with a hybrid LTQ-Orbitrap–Velos mass spectrometer (Thermo Fisher Scientific). Briefly, after trypsin digestion (12.5 ng/μl in 40 mmol/liter NH_4HCO_3–10% acetonitrile, overnight at 40°C), the peptides were loaded and washed on a C_{18} reverse-phase precolumn. The loading buffer contained 98% H_2O, 2% acetonitrile (ACN), and 0.1% trifluoroacetic acid (TFA). Peptides were then separated on a C_{18} reverse-phase resin with a 4-min effective gradient from 100% solvent A (0.1% formic acid and 100% H_2O) to 50% solvent B (80% ACN, 0.085% formic acid, and 20% H_2O).

The linear trap quadrupole-Orbitrap mass spectrometer acquired data throughout the elution process and operated in a data-dependent scheme, with full MS scans acquired with the Orbitrap mass spectrometer, followed by the acquisition of up to 20 LTQ MS/MS collision-induced dissociation spectra on the most abundant ions detected by the MS scan. Mass spectrometer settings were as follows: for full MS, automatic gain control (AGC) was 1×10^6, the resolution was 6×10^4, the *m/z* range was 400 to 2,000, and the maximum ion injection time was 500 ms; for MS/MS, AGC was 5×10^3, the maximum injection time was 50 ms, the minimum signal threshold was 500, the isolation width was 2 Da, and the dynamic exclusion time setting was 15 s. Precursors were fragmented with charge states of 2, 3, 4, and up. The signal-to-noise threshold for extraction values was 3.

Database searches were carried out using the Mascot server (version 2.2; Matrix Science, London, United Kingdom) on "other mammalia" from the Swiss-Prot databank (538,849 sequences, January 2013; www.expasy.org) and NCBInr databank (22,663,875 sequences, January 2013; http://www.ncbi.nlm.nih.gov/). The search parameters were as follows: carbamido methylation as a variable modification for cysteines and oxidation as a variable modification for methionines. Up to one missed tryptic cleavage was tolerated. The mass accuracy tolerance for all tryptic mass searches was 5 ppm for precursors and 0.45 Da for fragments. Positive identification was based on a Mascot score above the significance level (i.e., <5%). The reported proteins were always those with the highest number of peptide matches. With our identification criteria, no result was found to match multiple members of a protein family.

Nucleic acid extraction. Thirty milligrams of liver was disrupted as described before (29). Total RNAs from liver were extracted using an RNeasy minikit (Qiagen, Courtaboeuf, France). Viral RNAs were extracted from bile and fecal suspensions as described by Bouquet et al. (30).

RT and PCR controls. Precautions were taken to prevent false-positive and false-negative results in the RT-PCR amplification. In addition to spatial separation of work spaces at crucial experimental points (e.g., for RNA extraction and PCR mix preparation), each experiment included several control samples: positive samples for RNA extraction and negative and positive controls for RT and real-time PCR.

Quantification of HEV RNA by TaqMan RT-PCR. HEV RNA quantification was adapted from the method described by Jothikumar and collaborators (31) and performed as described in Barnaud et al. (32). Each sample was analyzed in duplicate.

Analysis of mRNA levels of candidate proteins by real-time PCR. cDNA synthesis was performed from 400 ng of total liver RNA at 42°C for 60 min with 2.5 μl of hexamer, 60 U of PrimeScript reverse transcriptase TaKaRa in RT buffer (Ozyme, St. Quentin en Yvelines, France), 1 mM deoxynucleoside triphosphate mix (Ozyme, St. Quentin en Yvelines, France), and 12 U of RNase inhibitor (Life Technologies, Villebon sur Yvette, France). The reverse transcriptase activity of PrimeScript reverse transcriptase TaKaRa was then heat inactivated at 72°C for 10 min. Primers specific for the gene of interest were designed with NCBI PrimerBlast software (http://www.ncbi.nlm.nih.gov/tools/primer-blast/): for GAPDH (glyceraldehyde-3-phosphate dehydrogenase), forward primer 5′-CACCATCTTCCAGGAGCGAG-3′ and reverse primer 5′-GAGATG ATGACCCTTTTGGC-3′; for ApoE, forward primer, 5′-GCCTTCAMC TCCTTCATGST-3′ and reverse primer 5′-CTTYTGGGATTACCYGCG CT-3′; for heterogeneous nuclear ribonucleoprotein K (HnRNPK), forward primer 5′-TCTGGGACTGAAACACTGGC-3′ and reverse primer 5′-TCAG AGCAAGAATGCTGGGG-3′; for prohibitin (PHB), forward primer 5′-CA CCACAAATCTGGCCCTCT-3′ and reverse primer 5′-AGGAGTTCACAG AAGCGGTG-3′; and for protein phosphatase 2A (PP2A), forward primer 5′-CCACAGCAAGTCACACATTGG-3′ and reverse primer 5′-CAGAGCA CTTGATCGCCTRCAA-3′.

Real-time PCR was performed using a SYBR green PCR kit (Qiagen, Courtaboeuf, France), according to the manufacturer's instructions, with 2 μl of cDNA (template). Reverse and forward primers for the gene of interest were used at a final concentration of 0.1 μM. A LightCycler PCR system (Roche Molecular Biochemicals, Meylan, France) was used for sample analysis according to the following steps: 30 s at 94°C and 45 cycles of denaturation at 94°C for 30 s, annealing for 30 s at 56°C, and an extension at 72°C for 30 s, followed by a final extension at 72°C for 10 min. Each sample was analyzed in duplicate. The data were submitted to quantitative analysis using the $2^{-\Delta\Delta CT}$ threshold cycle (C_T) method (33). Samples from the mock-infected group were used as the calibrator (relative expression, +1), and the GAPDH RNA gene was used as an internal reference gene. The test was performed in duplicate for each sample from three independent determinations.

Immunoblotting. Denatured proteins (50 μg) from each liver sample were separated by electrophoresis through a 10% SDS-polyacrylamide gel and transferred to a nitrocellulose membrane. After blocking for 2 h at room temperature with 5% (wt/vol) nonfat powdered milk in PBS with 0.05% Tween 20, the proteins of interest were detected using goat polyclonal anti-GAPDH (1/100; clone V18; catalog number sc-20357; Clinisciences, Nanterre, France), goat polyclonal anti-ApoE (1/700; catalog number AB947; Millipore, Molsheim, France), rabbit monoclonal anti-HnRNPK (1/500; clone EP943Y; catalog number ab52600; Abcam, Paris, France), or mouse monoclonal anti-prohibitin (1/100; catalog number MA512858 [II-14-10]; Thermo Fisher Scientific, Illkirch, France) over-

night at 4°C. The membranes were then incubated with horseradish peroxidase-conjugated goat anti-mouse IgG (1:3,000) or rabbit anti-goat Ig (1:5,000) or goat anti-rabbit Ig (1:5,000) for 1 h at room temperature (Dako, Les Ulis, France). Blots were developed by enhanced chemiluminescence (ECL; Amersham, Amersham-GE Healthcare Europe GmbH, Saclay, France) and scanned with a Fusion Fx5 solo system (Vilber Lourmat, Marne-la-Vallée, France). Bio-1D software was used for densitometric quantification. GAPDH was used as a reference protein. Triplicate analyses were performed for each sample.

Network modeling. The data sets for the proteins differentially expressed in liver mock infected and infected with HEV strain C were analyzed using Ingenuity Pathway analysis and Pathway Studio (version 9.0) software to identify molecular and cellular processes, high-level functions, disorders, and signaling pathways associated with gene regulatory networks.

RESULTS

Experimental infection and replication efficiency. Prior to inoculation, all the pigs tested negative for HEV antibodies and RNA (data not shown). After HEV inoculation, the presence of viral RNA in feces was monitored for 8 days p.i. Virus excretion in all pigs was detected from 3 days p.i. and reached a maximum of approximately 10^6 copies of HEV RNA/g of feces at 8 days p.i. (Fig. 1A). There was no significant difference in the kinetics of HEV fecal excretion in the infected animals in terms of the duration or quantity, whichever strain was used (Fig. 1A). The pigs were euthanized at 8 days p.i., and the bile and liver were collected from each animal.

HEV infection efficiency was evaluated by measuring the level of HEV RNA in the liver and bile of infected pigs. In the liver, the number of genome equivalents (GE) was slightly higher with strain A than with the other two strains. The median viral RNA level reached 5.4×10^6 GE · g^{-1} with strain A, whereas it was 4×10^5 GE · g^{-1} with strain B and 7.2×10^5 GE · g^{-1} with strain C (Fig. 1B). In contrast, no significant difference in the viral RNA level of strains A, B, and C was observed in bile samples, with median levels of 7.6×10^6 GE · ml^{-1}, 1.86×10^6 GE · ml^{-1}, and 1.81×10^6 GE · ml^{-1}, respectively, being detected (Fig. 1C).

Impact of HEV infection on liver histology and enzymatic activities. To evaluate the possible development of mild disease, liver tissue sections were analyzed. Most of the specimens, including the mock-infected liver, were affected by diffuse liver steatosis (Fig. 2Aa and Ab). In some infected and uninfected livers, minimal inflammatory infiltrates were observed, with a few portal areas being infiltrated principally by lymphocytes and histiocytes (Fig. 2Ac and Ad). Thus, histology analysis did not reveal any difference between infected and uninfected animal livers. Aspartate transaminase (AST) and alanine transaminase (ALT) levels are commonly measured to estimate liver injury. The median values of ALT and AST obtained for pigs infected with strain B (ALT, 46 IU/liter; AST, 56 IU/liter) were slightly higher than those obtained for pigs infected with strain C (ALT, 40 IU/liter; AST, 30 IU/liter) or pigs in the mock-infected group (ALT, 40 IU/liter; AST, 34 IU/liter) ($P < 0.05$) but not those obtained for pigs infected with strain A (ALT, 47 IU/liter; AST, 36 IU/liter) (Fig. 2B). The level of cholesterol did not significantly differ between mock-infected pigs (0.64 mmol/liter) and pigs in the infected groups (strain A, 0.82 mmol/liter; strain B, 0.83 mmol/liter; strain C, 0.84 mmol/liter) (Fig. 2C, left). In contrast, the median triglyceride levels obtained for pigs infected with strain C were significantly lower (0.32 mmol/liter) than those obtained for pigs infected with strain A (0.44 mmol/liter) and the mock-infected healthy controls (0.41 mmol/liter) ($P < 0.01$) but not the level obtained for pigs infected with strain B (0.39 mmol/liter). Overall, the enzymatic activities stayed in the normal range.

2D-DIGE analysis of infected and uninfected livers. To investigate the global protein changes in liver tissues after infection with different strains of HEV genotype 3, a 2D-DIGE analysis was performed (see Fig. S1 in the supplemental material). A total of four groups were analyzed: a mock-infected group (group T) and the groups infected with the three different strains: strain A, strain B, and strain C. In order to assess significant differential expression as a result of infection, multiple group-to-group comparisons were performed using computer-assisted analysis (DeCyder 2D [version 7.0] software; GE Healthcare) and revealed 153 differentially expressed spots (fold change, ≥ 1.5 or ≤ -1.5; Student's t test, $P < 0.05$). In comparison to the mock-infected group, 73 differentially expressed spots (58 upregulated and 15 downregulated) were detected in the gel with samples from the strain C-infected group, whereas 31 (13 upregulated and 18 downregulated) and 35 (19 upregulated and 16 downregulated) differentially expressed spots were detected in the gels with strain A and strain B, respectively (see Table S1 in the supplemental material).

To examine the global proteomic profile of each group and allow comparison of the groups, the data were subjected to principal component analysis (PCA) using all matched protein spots (Fig. 3). PCA revealed a pattern that clearly segregated the infected groups from the mock-infected group. The pattern of the strain C-infected group was distinct from that of the mock-infected group and the strain A- and B-infected groups (Fig. 3).

Protein identification of spots of interest. The 153 differential spots were excised and analyzed by matrix-assisted laser desorption ionization–time of flight/time of flight (MALDI-TOF/TOF) tandem mass spectrometry (MS) and LTQ-Orbitrap MS. One hundred two spots corresponding to 61 different proteins were successfully identified. A total of 24, 25, and 30 different proteins were identified with the strain A-, strain B-, and strain C-infected groups, respectively. Detailed information on the identified proteins is provided in Table 1. According to their expression level during HEV infection, the identified proteins were classified into two main groups. The first one comprised proteins which were upregulated, and the second group comprised proteins which were downregulated (Table 2). A functional classification based on annotations from the UniProt Knowledgebase was performed. The overexpressed proteins identified with strain B were mainly involved in metabolism (33%) or cholesterol/lipid metabolism (25%). The other proteins were implicated in toxicity/inflammatory/immune response (17%) and cytoskeleton/trafficking (18%). The downregulated proteins identified with strain B were principally involved in the same functions: metabolism (36%) and toxicity/inflammatory/immune response (27%) (Table 2). With strain A, the overexpressed proteins were mostly involved in metabolism (47%), toxicity/inflammatory/immune response (27%), and cytoskeleton/trafficking (18%). No upregulation of a protein involved in transcription/transcription regulation was identified with strain A (Table 2). Downregulated proteins identified with strain A mainly concerned metabolism (42%), chaperone proteins (17%), and toxicity/inflammatory/immune response (17%) (Table 2). The upregulated proteins identified with strain C were distributed into the eight functional groups: metabolism (43%), cholesterol/lipid metabolism (13%), cytoskeleton/trafficking (13%), signaling pathways

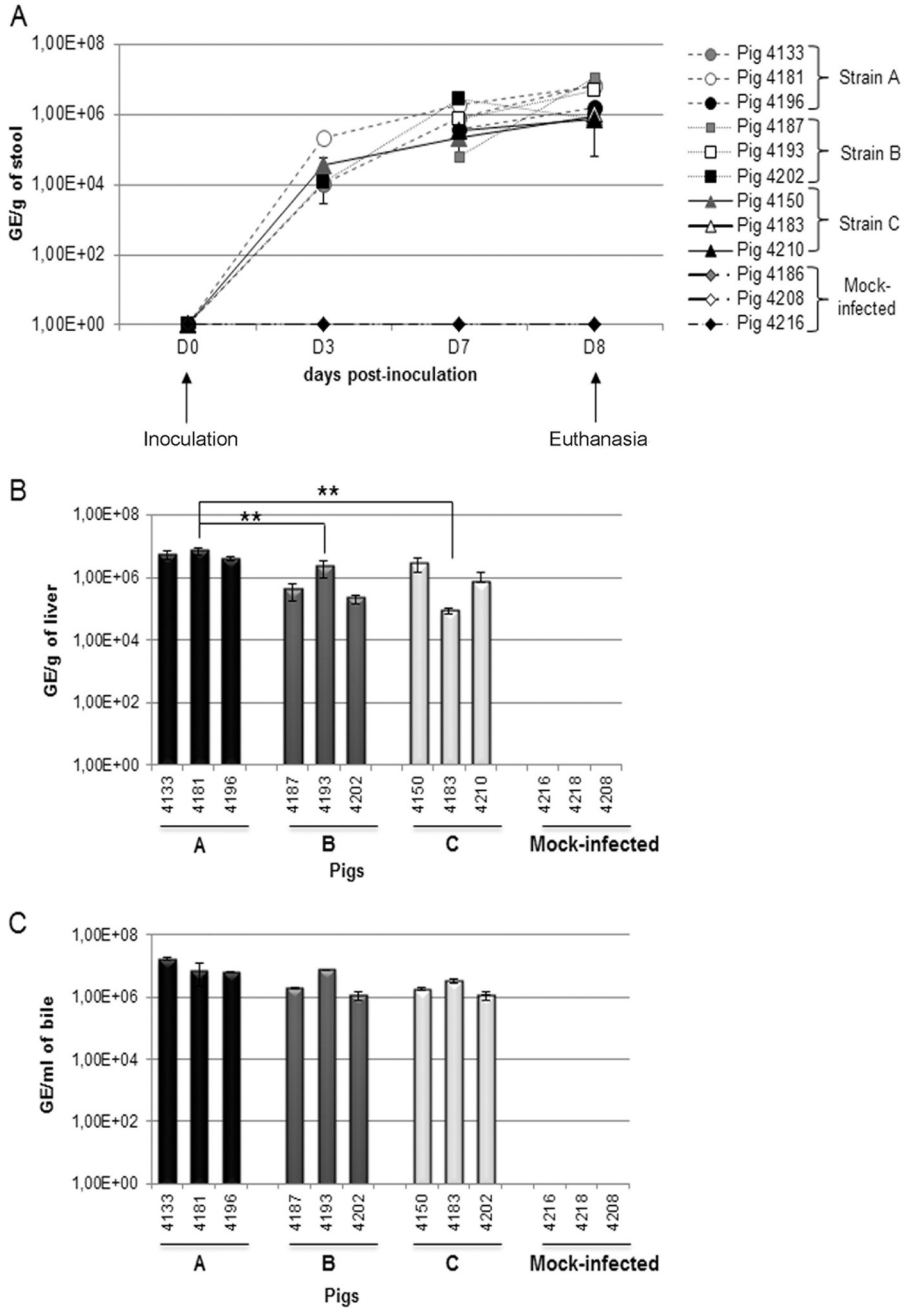

FIG 1 (A) Kinetics of HEV fecal excretion and viral multiplication. HEV excretion in fecal samples was quantified by real-time RT-PCR. The times of inoculation and euthanasia and the day (D) postinoculation are indicated on the axis. (B and C) The liver and bile of infected- or mock-infected pigs were collected at 8 days p.i. The HEV RNA present in the liver (B) or bile (C) was quantified by real-time RT-PCR. Results are expressed as the average number of HEV RNA copies per g or ml of sample ± standard error of the mean from three independent experiments. **, significant difference ($P < 0.01$) in HEV RNA levels.

(9%), cell proliferation (9%), chaperone proteins (4%), transcription/transcription regulation (4%), and toxicity/inflammatory/immune response (4%). The downregulated proteins identified with strain C were mainly involved in metabolism (22%), cholesterol/lipid metabolism (22%), chaperone proteins (22%), signaling pathways (11%), cytoskeleton/trafficking (11%), or toxicity/inflammatory/immune response (11%) (Table 2).

Validation of proteomic data using immunoblotting and qRT-PCR. To validate the results obtained using the proteomic approach, the expression levels of three proteins upregulated with all three HEV strains—heterogeneous nuclear ribonucleoprotein K (HnRNPK), apolipoprotein E (ApoE), and prohibitin (PHB)—were quantified after immunoblotting (Fig. 4A). GAPDH was used as the loading control. The result showed an increase in the abundance of the proteins HnRNPK and PHB in all the infected groups. In contrast, the abundance of ApoE increased only in the groups infected with strains B and C. The densitometric analysis of each immunoblot revealed fold changes for strains A, B, and C

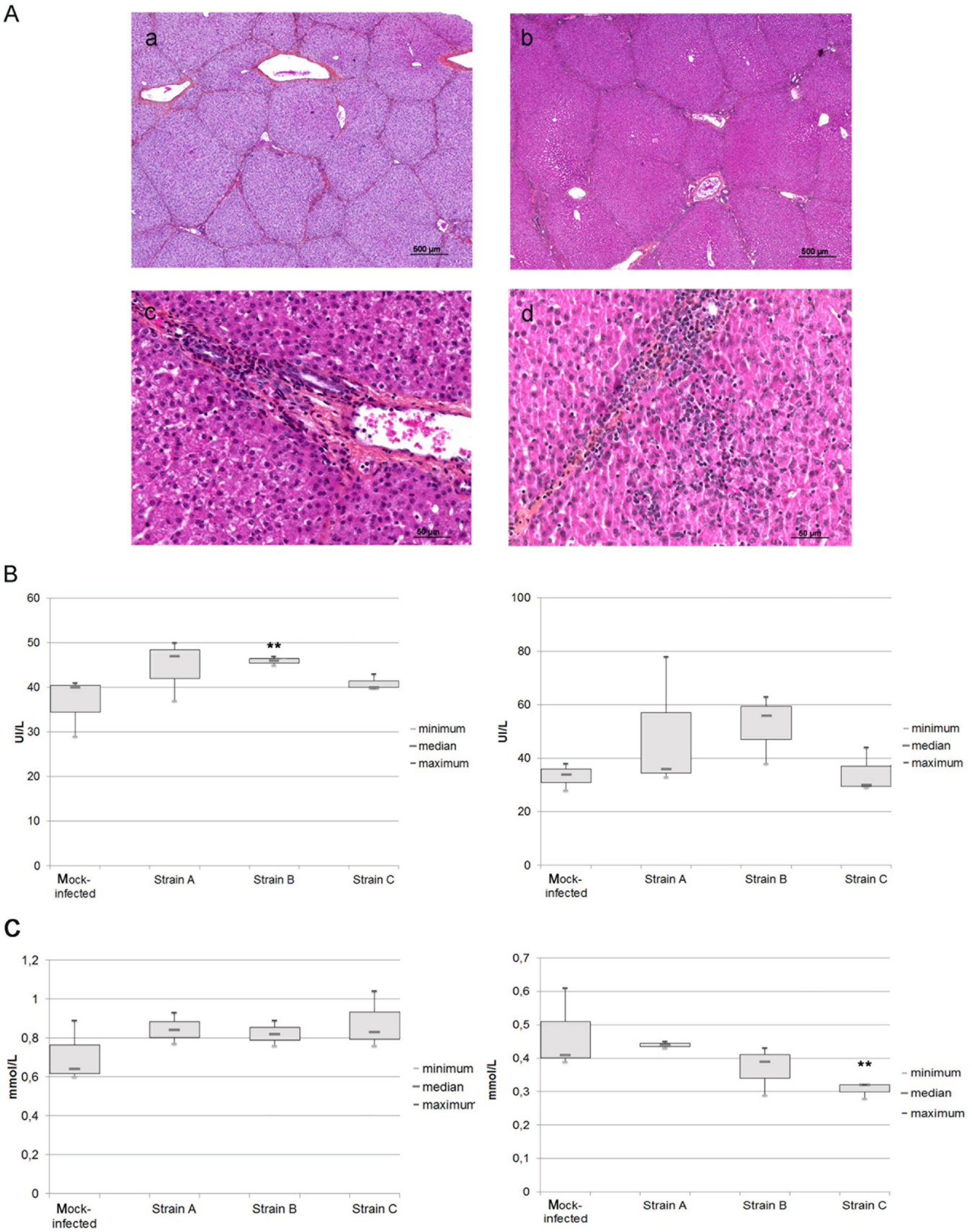

FIG 2 Histopathology and biochemical analysis. (A) Representative microphotographs of sections of HEV-infected or uninfected liver tissue. The tissue was stained with hematoxylin and eosin. (a) Normal aspect; (b) marked diffuse steatosis; (c and d) inflammatory lymphocytic and histiocytic infiltrates in portal areas; (a, b, c) infected liver; (d) mock-infected liver. Magnifications, ×200. (B and C) AST (B, right) and ALT (B, left) activities and cholesterol (C, left) and triglyceride (C, right) levels in the serum of the mock-infected and infected groups at 8 days postinoculation. The data represent the medians and minimum and maximum values obtained for three pigs in each group. UI, international units. *, $P < 0.05$ compared to mock-infected pigs; **, $P < 0.01$ compared to mock-infected pigs.

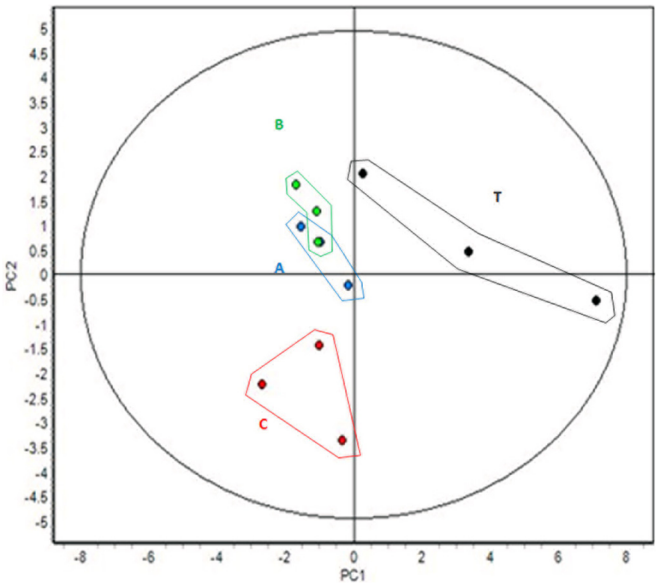

FIG 3 PCA performed from all spots detected and matched (2,117 spots). The score plot shows experimental spot maps.

of 1.8, 1.6, and 1.8, respectively, for HnRNPK; 1.3, 1.6, and 1.7, respectively, for ApoE; and 1.3, 1.4, and 1.5, respectively, for PHB (Fig. 4B). The results were comparable to the fold changes observed by 2D-DIGE analysis, which were, with strains A, B, and C, 1.6, 1.8, and 1.6, respectively, for HnRNPK; 1.3, 1.6, and 1.7, respectively, for ApoE; and 1.3, 1.2, and 2.2, respectively, for PHB (Table 1).

To further validate the upregulation of two proteins observed with strain C—PHB and protein phosphatase 2A (PP2A)—and the upregulation of two proteins observed with strains B and C—ApoE and HnRNPK—the quantity of their RNA transcripts was measured by qRT-PCR. As shown in Fig. 4C, the mRNA levels of these four genes were upregulated in all infected groups. The results showed that the mRNA fold changes of HnRNPK and PP2A were comparable for strains A, B, and C: for HnRNPK, 2.2, 2, and 2.3, respectively, and for PP2A, 1.9, 2, and 2.3, respectively. However, the mRNA level of PHB was higher with strain C than with the other two strains (strain A, 1.8; strain B, 1.8; strain C, 2.5). In addition, infection with strains B and C resulted in a stronger upregulation of the mRNA of ApoE than infection with strain A (mRNA levels, 1.6, 3.1, and 2.2 for strains A, B, and C, respectively). In comparison with the data obtained by 2D-DIGE analysis, the trends in the mRNA levels of these genes were not completely consistent with the fold change in the levels of their corresponding proteins. Nevertheless, it is known that mRNA expression does not always correlate with the level of protein expression.

Analysis of interaction networks. Strain C corresponds to a phylogenetic cluster frequently associated with viral hepatitis E in Europe (80% in France), and this strain showed the greatest number of proteins differentially expressed in this proteomic analysis. Thus, the interaction networks were modeled from the data set obtained with strain C. The cellular and disease processes associated with the differentially expressed proteins were determined using Pathway Studio (version 5.0) software (Fig. 5). In addition to sterol biosynthesis and cholesterol metabolism, the identified proteins—such as HnRNPK, PHB, ApoE, and apolipoprotein A-IV (ApoA-IV)—are known to be involved in viral diseases, liver cirrhosis, neuron toxicity, and neurodegenerative diseases. The different cell processes identified were directly or indirectly linked to networks involving four major transcription factors: signal transducer and activator of transcription 3 (STAT3), hepatocyte nuclear factor 4 alpha (HNF4A), peroxisome proliferator-activated receptor gamma (PPARγ), and sterol regulatory element-binding transcription factor 1 (SREBF-1). To further analyze the relationship between the known cellular pathways and hepatitis E virus infection, a network was built using the Ingenuity Pathway system. The results showed that 17 proteins, approximately the same number obtained with Pathway Studio software, could be connected in a network. Transcription factors SREBF-1, PPARγ, E2F1, and FOS and the extracellular signal-regulated kinases (ERKs), nuclear factor kappa B (NF-κB), and Akt cascade signaling were linked to the proteins differentially expressed during HEV infection (Fig. 6).

DISCUSSION

The clinical symptoms associated with HEV infection vary widely, ranging from a flu-like syndrome, nausea, and jaundice to chronic infection with possible evolution to fibrosis, cirrhosis, or neurological disorders and even fatal fulminant hepatitis. To understand these clinical manifestations, there are very sparse data on HEV biology and pathogenesis. In the swine model of HEV infections, animals do not exhibit clinical signs, but in humans as well, many cases are probably asymptomatic (5). During HEV infection of swine, the virus replicates profusely in the liver and is abundantly shed in the feces. Although HEV is eliminated by the immune system, it hijacks the cellular machinery for its replication, affecting cellular functions. Thus, the infection of swine hepatocytes can be used as a cellular model to identify cellular pathways modulated during HEV infection. Some phylogenetic clusters of HEV strains are more frequently observed in human and swine populations, so the factors modulated during infection with strains belonging to different clusters (less than 90% nucleotide sequence identity over the full-length genome) were evaluated.

The present study confirms that during hepatitis E virus infection of swine, global liver functions remain intact without lymphoplasmacytic inflammation or focal necrotic hepatocytes and with normal values for ALT, AST, cholesterol and triglycerides. The replication efficacy of the three different strains was similar in terms of the duration of HEV shedding and the quantity of HEV secreted in the stool and bile of all infected animals. However, the level of HEV RNA in the liver was statistically significantly higher with strain A than with strains of the other subtypes, suggesting better replication. However, since no increase in the corresponding bile and fecal samples was observed, this might be due to sampling bias induced by biopsy localization.

Despite the absence of an increase in cholesterol levels in infected animals, the proteomic analysis of HEV-infected livers showed that cholesterol and lipid metabolism was modulated during infection, whatever the strain used. Furthermore, ApoE—which is known to play an important role in the transport of lipids in the plasma—was upregulated with infection with strains B and C. The secretion pathway taken by the HEV virion is not well understood, but ApoE has been shown to be involved in the propagation and release of HCV (34). HEV particles are secreted into the intestinal lumen via the bile duct. Different studies have shown

TABLE 1 Overview of proteins differentially expressed in the liver of a pig during HEV infection

Protein description[a]	Accession no.[b]	Strain A		Strain B		Strain C	
		P value[c]	Fold change[c,d]	*P* value	Fold change	*P* value	Fold change
Agmatinase, mitochondrion-like	gi|311258562	*1.2E−02*	*1.4*	**5.2E−04**	**1.5**	*2.6E−01*	*1.3*
Alpha-1-antichymotrypsin 2	gi|9968805	*2.5E−01*	*2.0*	**4.1E−03**	**1.9**	*5.7E−01*	*−1.2*
Alpha-1-antichymotrypsin 2 precursor	gi|47523270	*4.3E−01*	*−1.4*	**1.3E−03**	**−2.6**	*3.8E−01*	*−1.4*
Alpha-2-macroglobulin	gi|417515493	*2.3E−01*	*−1.9*	**1.2E−02**	**−2.2**	*5.3E−02*	*−2.1*
Alpha-enolase-like, partial	gi|350585579	*6.3E−02*	*−1.4*	**1.6E−02**	**−1.6**	*2.1E−01*	*−1.1*
Cathepsin Z precursor (*Sus scrofa*)	gi|178057125	*4.7E−02*	*1.4*	**8.9E−03**	**1.6**	*7.6E−02*	*1.3*
Glutamine synthetase	GLNA_PIG	**1.9E−02**	**−2.0**	**2.1E−03**	**−1.7**	**1.2E−02**	**−2.2**
Heterogeneous nuclear ribonucleoprotein K	gi|392513715	*2.2E−01*	*1.6*	**1.2E−02**	**1.8**	**7.1E−03**	**1.6**
Indolethylamine *N*-methyltransferase	gi|347800713	**3.0E−02**	**−1.7**	**1.1E−02**	**−1.5**	*1.2E−01*	*−1.3*
Phosphoglucomutase-2 and mitochondrial inner membrane protein, partial		**3.7E−02**	**1.6**	**1.3E−02**	**1.8**	**8.3E−03**	**2.0**
Serotransferrin	TRFE_PIG	*1.1E−01*	*−1.4*	**1.6E−02**	**−1.5**	*2.9E−01*	*−1.3*
Serpin A3-8, partial	gi|350587171	*3.3E−01*	*−1.4*	**8.2E−03**	**−1.9**	*6.4E−01*	*−1.1*
Serpin A3-8, partial	gi|350587171	*2.1E−01*	*1.9*	**3.0E−03**	**2.0**	*7.6E−01*	*1.0*
Vimentin-like (*Sus scrofa*)	gi|335296459	*4.7E−01*	*−1.6*	**3.3E−03**	**−4.4**	*3.9E−01*	*−1.6*
Collagen alpha-2(VI) chain	gi|335300861	**2.4E−02**	**−1.8**	*8.6E−02*	*−1.5*	*1.9E−01*	*−1.5*
3-Hydroxy-3-methylglutaryl-CoA synthetase 1	gi|356582301	**2.6E−02**	**−1.8**	**4.1E−02**	**−1.6**	**1.3E−02**	**−2.3**
3-Hydroxyisobutyrate dehydrogenase, mitochondrial	3HIDH_BOVIN	**1.4E−02**	**1.5**	*3.5E−01*	*1.3*	*3.0E−01*	*1.4*
4-Trimethylaminobutyraldehyde dehydrogenase	gi|194036835	*1.7E−01*	*1.2*	*5.2E−02*	*1.3*	**7.3E−05**	**2.4**
Actin, cytoplasmic 1	ACTB_PIG	*1.1E−01*	*1.1*	*1.8E−01*	*1.1*	**5.5E−03**	**1.5**
Aminoacylase-1	ACY1_PIG	**1.6E−02**	**−1.7**	**1.8E−02**	**−1.5**	*9.2E−03*	*−1.4*
Apolipoprotein A-IV	APOA4_PIG	**3.4E−02**	**1.7**	*2.7E−01*	*1.5*	**1.5E−03**	**2.5**
Apolipoprotein A-IV	APOA4_PIG	*4.3E−02*	*1.3*	**4.0E−02**	**1.6**	**2.6E−02**	**2.7**
Apolipoprotein E	APOE_PIG	*3.2E−01*	*1.3*	**2.3E−02**	**1.6**	**1.5E−02**	**1.7**
Carbamoyl-phosphate synthase (ammonia), mitochondrial isoform 1	gi|350593858	*1.2E−01*	*−1.3*	*7.5E−01*	*−1.1*	**7.7E−03**	**2.5**
Cathepsin D	CATD_PIG	*5.5E−02*	*1.3*	*3.2E−02*	*1.3*	**1.3E−03**	**1.5**
Cytosolic beta-glucosidase-like, partial	gi|350587405	**1.2E−02**	**2.1**	*4.2E−03*	*1.4*	*7.1E−01*	*1.2*
Diamine acetyltransferase 2	SAT2_PIG	**1.9E−02**	**−1.5**	*6.2E−02*	*−1.4*	*5.2E−02*	*−1.4*
Epoxide hydrolase 2	HYES_PIG	**9.3E−03**	**1.7**	*3.6E−01*	*1.4*	*8.6E−01*	*1.2*
Gamma interferon-inducible lysosomal thiol reductase	GILT_PIG	**1.0E−02**	**1.6**	*1.9E−02*	*1.4*	*2.8E−01*	*1.2*
Golgi reassembly-stacking protein 2 isoform 1	gi|335302969	*1.5E−01*	*1.4*	*9.1E−02*	*1.4*	**2.2E−02**	**1.6**
Golgi reassembly-stacking protein 2 isoform 1	gi|335302969	*9.2E−02*	*1.3*	**2.1E−02**	**1.7**	*2.6E−02*	*1.5*
Heat shock protein beta-1	HSPB1_PIG	*2.7E−01*	*1.2*	*1.9E−02*	*1.4*	**2.8E−03**	**1.6**
Heat shock protein beta-1	HSPB1_PIG	*1.3E−01*	*−1.2*	*1.2E−01*	−1.4	**2.6E−02**	**−1.6**
Heat shock protein beta-1	HSPB1_PIG	*9.2E−02*	*−1.6*	**2.4E−02**	**−2.0**	5.1E−02	−2.2
Heat shock protein HSP90-alpha	HS90A_PIG	*4.0E−02*	*−1.4*	*6.3E−01*	*−1.1*	**1.1E−02**	**−1.5**
Hemoglobin subunit beta	HBB_PIG	**3.2E−02**	**1.6**	**2.1E−02**	**1.5**	*3.7E−01*	*1.1*
Hepatoma-derived growth factor-like	gi|335286747	*4.7E−01*	*1.2*	*3.3E−01*	*1.6*	**1.0E−02**	**2.2**
Isopentenyl-diphosphate delta-isomerase 1-like	gi|335296666	*3.8E−02*	*−1.3*	*2.5E−02*	*−1.4*	**2.1E−02**	**−1.6**
Liver carboxylesterase	EST1_PIG	**2.2E−02**	**−1.7**	*7.8E−02*	*−1.5*	**4.4E−02**	**−1.6**
Liver carboxylesterase	EST1_PIG	**4.8E−02**	**−2.3**	*1.1E−01*	*−2.1*	*6.8E−02*	−1.8
L-Lactate dehydrogenase B chain	LDHB_PIG	**2.6E−02**	**−1.7**	*1.1E−02*	*−1.4*	*5.1E−02*	*−1.4*
Peptidyl-prolyl *cis-trans* isomerase FKBP4	gi|305855148	**2.0E−02**	**−1.6**	*4.3E−01*	*−1.2*	*3.8E−01*	*−1.1*
Phosphoenolpyruvate carboxykinase (GTP), mitochondrial	gi|330417958	**3.5E−02**	**2.0**	*1.1E−01*	*1.8*	*3.0E−01*	*1.4*
Phosphoenolpyruvate carboxykinase, cytosolic	gi|178056560	*3.9E−01*	*1.4*	*1.3E−01*	*2.0*	**4.5E−03**	**2.7**
Poly(ADP-ribose) glycohydrolase ARH3-like	gi|311258899	*5.7E−01*	*1.1*	*5.4E−01*	*1.6*	**2.3E−02**	**2.5**
Probable imidazolonepropionase	gi|335288858	**3.0E−02**	**−2.1**	*1.1E−01*	*−1.7*	**4.3E−02**	**−1.7**
Prohibitin-like	gi|350590415	*2.7E−01*	*1.3*	*1.6E−01*	*1.2*	**7.2E−03**	**2.2**
Protein kinase	gi|984249	**4.5E−02**	**1.5**	**1.9E−02**	**1.6**	*5.0E−01*	*1.4*
Protein kinase	gi|984249	*9.5E−02*	*−1.3*	*8.9E−01*	*−1.0*	**4.4E−02**	**−1.5**
Protein kinase	gi|984249	*9.7E−02*	*1.3*	*3.3E−01*	*1.4*	**2.7E−03**	**2.8**
Pyruvate kinase isozymes R/L-like	gi|350597093	*2.7E−01*	*1.7*	**3.6E−02**	**1.5**	*6.2E−02*	*1.4*

(Continued on following page)

TABLE 1 (Continued)

Protein description[a]	Accession no.[b]	Strain A		Strain B		Strain C	
		P value[c]	Fold change[c,d]	*P* value	Fold change	*P* value	Fold change
Retinol-binding protein 4	RET4_PIG	*1.0E−01*	*1.4*	*4.4E−02*	*1.3*	**2.3E−02**	**1.7**
Ribokinase/actin, cytoplasmic 1	gi|351738777/ACTB_PIG	**4.0E−02**	**1.5**	*3.5E−01*	*1.1*	*4.9E−02*	*1.4*
Serine/threonine-protein phosphatase 2A 65-kDa regulatory subunit A beta isoform (fragment)	2AAB_PIG	*3.3E−01*	*1.3*	*8.7E−03*	*1.4*	**3.4E−03**	**1.5**
Serum albumin	ALBU_PIG	*7.6E−02*	*−1.7*	**1.3E−02**	**−1.7**	*1.8E−01*	*−1.4*
Serum albumin	ALBU_PIG	*3.0E−01*	*1.7*	*3.0E−01*	*1.3*	**2.7E−03**	**4.4**
Short/branched-chain-specific acyl-CoA dehydrogenase, mitochondrial or adipocyte plasma membrane-associated protein-like	gi|311271975/gi|350594715	*1.3E−01*	*1.2*	**3.7E−02**	**1.5**	*6.0E−02*	*1.2*
Short-chain-specific acyl-CoA dehydrogenase, mitochondrial	ACADS_PIG	*5.9E−02*	*1.6*	*5.3E−02*	*1.3*	**1.2E−02**	**2.1**
Stress-induced-phosphoprotein 1-like	gi|335281609	**2.1E−02**	**−1.8**	*7.3E−01*	*−1.1*	*6.8E−01*	*−1.1*
Succinate dehydrogenase	DHSA_PIG	*1.9E−01*	*1.2*	*7.3E−02*	*1.4*	**4.6E−02**	**1.5**
Tetranectin-like isoform 2	gi|335298955	*1.5E−01*	*−1.3*	*1.9E−01*	*−1.4*	**4.3E−03**	**−1.6**
Threonine synthase-like 1-like	gi|335296548	*2.8E−01*	*1.5*	*1.2E−01*	*1.3*	**4.2E−02**	**1.7**
trans-1,2-Dihydrobenzene-1,2-diol dehydrogenase	DHDH_PIG	*2.7E−01*	*1.3*	*3.5E−01*	*1.2*	**5.0E−03**	**1.6**
Type VI collagen alpha-1 chain	gi|335310813	**4.4E−02**	**−2.1**	*4.1E−01*	*−1.3*	*5.0E−01*	*−1.3*
Ubiquitin/ISG15-conjugating enzyme E2 L6	gi|350539097	**2.8E−02**	**1.6**	*9.4E−01*	*1.0*	*6.2E−01*	*−1.1*
Uncharacterized protein C2orf72-like	gi|350593962	**3.4E−02**	**−1.5**	*7.7E−02*	*−1.3*	*1.6E−01*	*−1.4*
Valacyclovir hydrolase precursor or alcohol dehydrogenase 1C (class I), gamma polypeptide	gi|343488509/gi|345441792	*5.5E−01*	*1.6*	*1.0E−01*	*1.3*	**3.1E−02**	**3.0**

[a] The name of the protein in the Swiss-Prot or NCBInr database.
[b] The accession number is the Mascot result of MALDI-TOF/TOF MS found in the Swiss-Prot or NCBInr database.
[c] The significant fold change and *P* values with *P* values of <0.05 are in bold, and insignificant fold change and *P* values are indicated in italics.
[d] Fold change between infected and control livers. Positive fold change values represent upregulation, whereas negative fold change values indicate downregulation of identified proteins.

that viral particles detected in the culture supernatant of infected cells (HepG2/C3A, A549, and PLC/PRF5 cells) and in the serum of infected patients appear to be associated with lipids (12, 35). It is possible that the secretion of new HEV progeny virions involves some hepatocyte transporter proteins involved in the secretion of biliary lipids, as in the case of HCV, hepatitis A virus, and flavivirus (36–38). In addition, ApoE has been shown to play a role as an immunomodulatory agent in the immune response and to be involved in neurodegenerative diseases, such as Alzheimer's disease and Guillain-Barré syndrome (39–41). HEV infection has been associated with several neurological symptoms (42), and ApoE could play a role in HEV pathogenesis. Modulation of proteins from the lipocalin family (retinol binding protein) was observed. They are involved in different functions, such as retinol transport, the immune response, and regulation of cell homeostasis (43). The modulation of lipid metabolism and proteins from the lipocalin family confirms the findings of previous investigations performed by Taneja and collaborators which analyzed the proteins and peptidome of the plasma or urine from patients with acute hepatitis E (44, 45).

Some proteins involved in glycolysis (pyruvate kinase, phosphoenolpyruvate carboxykinase), the urea cycle (carbamoyl-

TABLE 2 Functional classification of proteins differentially expressed during hepatitis E infection[a]

Functional classification	% proteins[b]: Upregulated			Downregulated		
	Strain A	Strain B	Strain C	Strain A	Strain B	Strain C
Metabolism	47	33	43	42	36	22
Transcription/transcription regulation	0	8	4	0	9	0
Cell proliferation	0	0	9	0	0	0
Cholesterol/lipid metabolism	9	25	13	8	9	22
Signaling pathways	9	8	9	0	0	11
Chaperone proteins	0	0	4	17	9	22
Cytoskeleton/trafficking	18	8	13	17	9	11
Toxicity/inflammatory/immune response	27	17	4	17	27	11

[a] The differentially expressed proteins listed in Table 1 were categorized according to their function reported in the literature.
[b] The numbers represent the percentage of identified proteins categorized in the indicated functional classification for each strain of HEV tested when their expression was compared to that in the control group (group T).

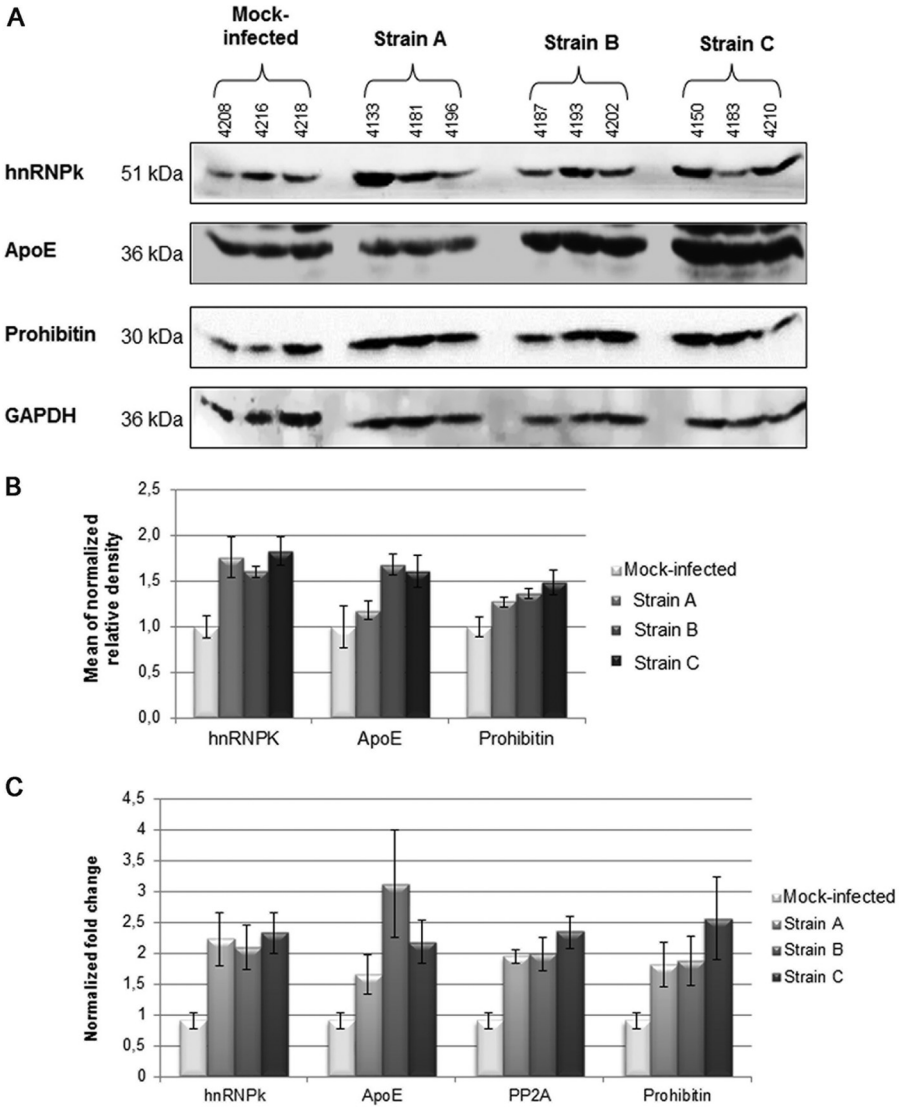

FIG 4 Detection and quantification of candidate proteins by immunoblotting or mRNA quantification. (A) The expression levels of HnRNPK, ApoE, and prohibitin were analyzed by immunoblotting. (B) Densitometric analysis of protein expression was performed using Bio-1D software. GAPDH was used as the internal control. Mean values ± standard errors of the means were calculated from three independent experiments and three biological replicates. (C) Transcript analysis by real-time RT-PCR of four proteins (HnRNPK, ApoE, PP2A, PHB) differentially expressed in HEV-infected livers. Data represent the median for three biological replicates per group and the average ± standard error from three independent experiments. The levels of expression in the samples were normalized by the level of expression of the GAPDH gene.

phosphate synthetase), the tricarboxylic acid cycle (succinate dehydrogenase, short-chain specific acyl coenzyme A [acyl-CoA] dehydrogenase), and amino acid metabolism (3-hydroxyisobutyrate dehydrogenase, threonine synthase, etc.) were identified. A previous study showed deregulation of these metabolic cycles and deregulation of amino acid metabolism in the plasma and urine of hepatitis E patients (46). In contrast to those results, a decrease in the level of lactate dehydrogenase was observed here, suggesting an absence of lactic acidosis in swine during hepatitis E virus infection. In the same way, Munshi et al. (46) reported decreased levels of ornithine and fumarate in the plasma of patients with hepatitis E, suggesting anomalies in ammonia detoxification. In the present study, the levels of expression of carbamoyl phosphatase, involved in the urea cycle, and succinated dehydrogenase, which converts succinate to fumarate, were increased in the liver of infected swine, suggesting an important ammonia detoxification. These differences might be explained by the type of tissues analyzed (liver tissues versus plasma or urine) and the species analyzed (swine versus human). Moreover, during swine experimental infection, no clinical symptoms were observed, whereas the patients had acute viral hepatitis E.

The Ingenuity Pathway analysis identified signaling pathways, such as the ERK, Akt, and NF-κB pathways, which have been shown to play a role in HEV replication (47–49). Indeed, it was shown previously that HEV ORF3 modulated the ERK activation and Akt pathways, promoting cell survival and viral multiplication (47–49). Furthermore, HEV ORF2 seemed to inhibit NF-κB, contributing to evasion of the host immune response at an early stage (47–49). In addition, the present study has shown that some transcription factors, such as STAT3, hepatocyte nuclear factor 4

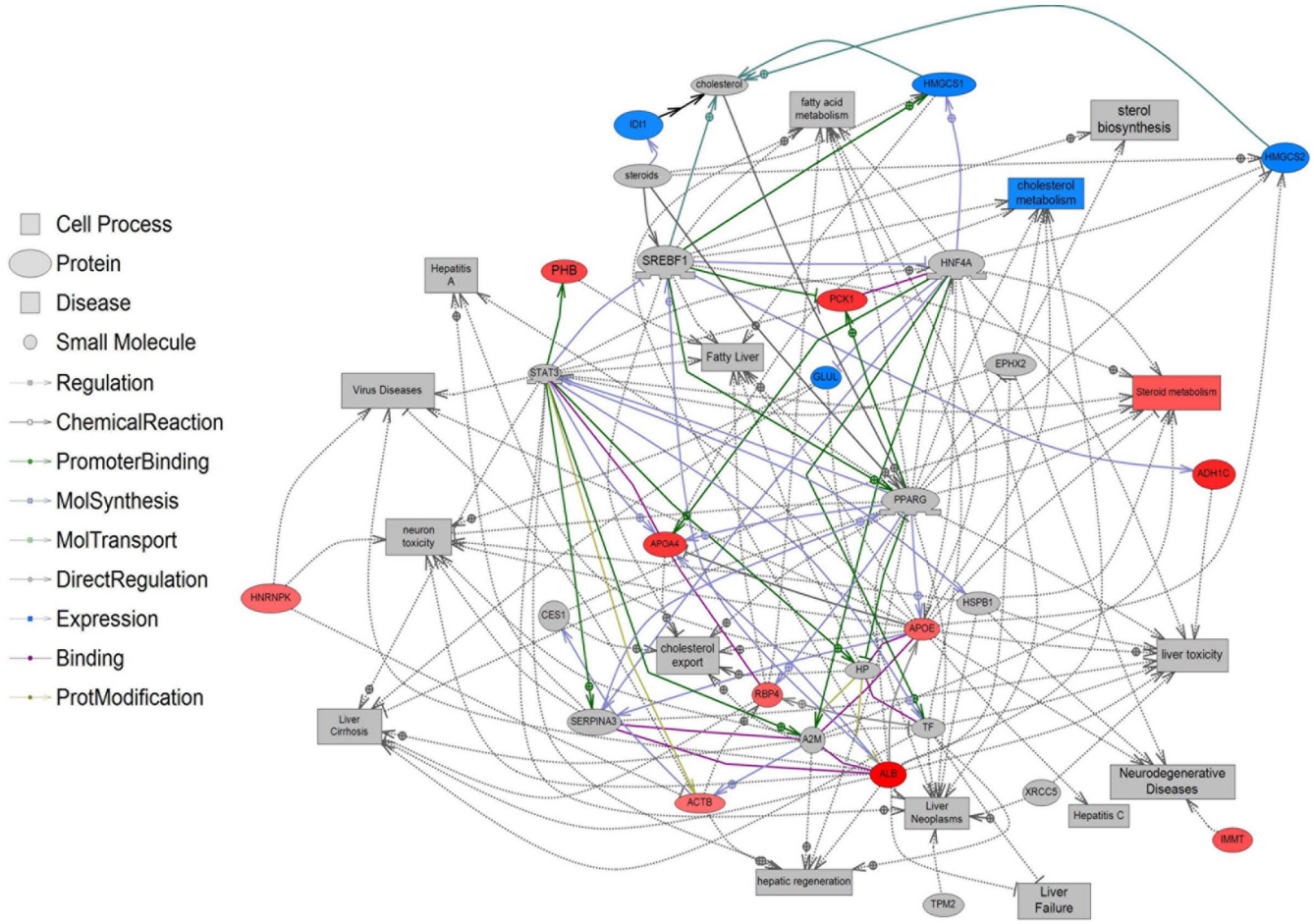

FIG 5 Interaction network and functional connectivity of proteins differentially expressed during infection with HEV strain C. Candidate proteins whose expression is modulated during HEV strain C infection (Table 1) were imported into Pathway Studio software, and the cellular networks impacted were generated. The key for the interaction network is provided in on the left. Mol, molecular; Prot, protein. Red, overexpressed proteins; blue, downregulated proteins.

(HNF4), sterol regulatory element-binding transcription factor 1 (SREBF-1), and peroxisome proliferator-activated receptor gamma (PPARγ), are probably impacted by HEV infection. The nuclear translocation of STAT3, which regulates the expression of genes for acute-phase proteins, and HNF4, which is involved in metabolism, blood maintenance, immune function, liver differentiation, and expression of growth factors (for a review, see reference 50), has been shown to be decreased by the ORF3 protein. The inhibition of STAT3 and HNF4 translocation may contribute to the survival of infected cells and successful HEV replication (51, 52). SREBF-1 and PPARγ both regulate the expression of a variety of genes involved in lipogenesis (53), lipid synthesis, transport, and storage in hepatocytes. Both SREBF-1 and PPARγ are upregulated in patients with chronic hepatitis B and hepatitis C. Upregulation of these proteins induces hepatic lipid accumulation, corresponding to a progression toward liver injuries, such as hepatitis (54, 55). The link between SREBF-1 and PPARγ and the list of proteins differentially expressed at an early stage of infection (8 days p.i.) suggest that HEV could induce mild hepatitis in swine at a later stage. Indeed, such an observation has already been made in genotype 3-infected swine at 20 days p.i. (56). Moreover, it was noted that in immunosuppressed humans infected with HEV, chronic hepatitis occurs and progresses into cirrhosis (57).

HnRNPK was also found to be upregulated in the present study. This factor contributes to several cell transcription steps, such as mRNA transport, RNA splicing, and direct transcriptional activity (58). Moreover, this protein has been shown to enhance the infection with several viruses by interacting either with a viral genome, such as with the genome of HCV (59–61), HBV (62), enterovirus 71 (63), or influenza A virus (64), or with viral proteins to support viral egress, such as with human herpesvirus 6 proteins (18). It would be interesting to further analyze the role of HnRNPK in the HEV replication cycle. Unfortunately, in the absence of a robust model for HEV culture *in vitro*, these studies will be delayed. The overexpression of PHB and PP2A was observed first with strain C, but their quantification by immunoblot analysis or determination of their mRNA levels revealed that they were upregulated with all three HEV strains. This small discrepancy might be due to a lesser sensitivity of the 2D-DIGE analysis. PHB has already been identified to be a receptor protein, mediating dengue virus serotype 2 or Chikungunya virus entry (65, 66), and is upregulated in HCV- or influenza virus-infected cells (67, 68). PHB is a member of the membrane protein superfamily and is involved in maintaining mitochondrial protein stability. It also contributes to the regulation of cell proliferation and plays a protective role against the induction of apoptosis (for a review, see

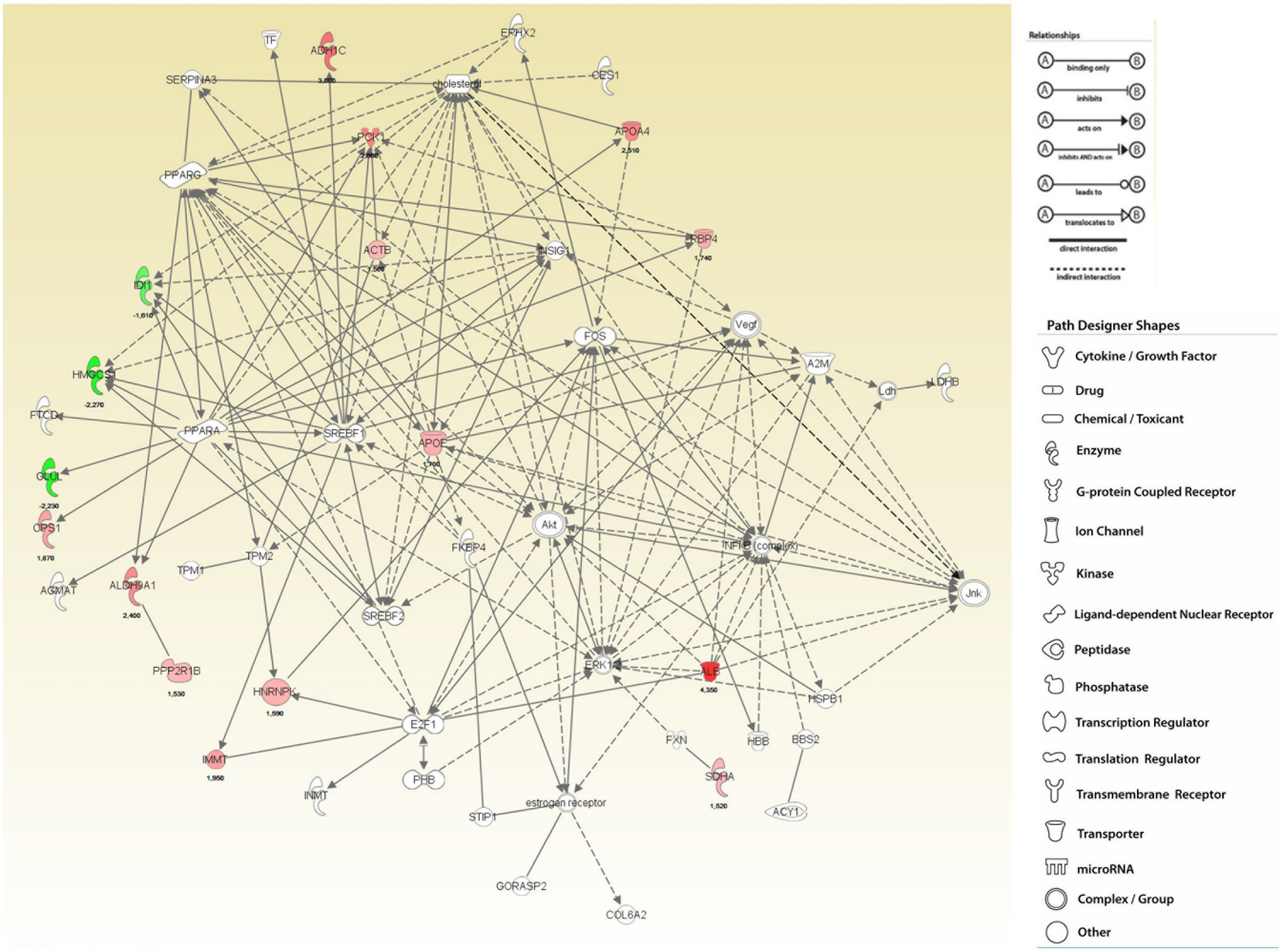

FIG 6 Signaling network of proteins differentially expressed during infection with HEV strain C. Candidate proteins whose expression is modulated during HEV strain C infection (Table 1) were imported into the Ingenuity Systems program, and networks of protein interactions were generated. Genes or gene products are represented as nodes, and the biological relationship between two nodes is represented by an arrow. A solid arrow denotes a direct relationship between two nodes, and a dashed arrow indicates an indirect relationship. Red nodes, upregulated proteins; green nodes, downregulated proteins. The different shades of red and green reflect the relative fold change.

reference 69). Several viruses interact with or deregulate PP2A expression in order to create a beneficial environment for the viral life cycle (for a review, see reference 70). HCV induces the upregulation of PP2A *in vitro* and *in vivo*, leading to the inhibition of alpha interferon-induced Jak-STAT signaling (71). It is possible that the overexpression of PHB and PP2A may contribute to HEV multiplication by reducing the inflammatory response and preventing cell apoptosis. Nevertheless, further investigations will be necessary to better understand the possible role of these proteins in the replication and pathogenesis of HEV.

A similar proteomic analysis of HEV-infected liver in swine was performed by Lee and collaborators using another strain of HEV (a phylogenetic cluster different from the phylogenetic clusters of strains A through C) (26). In comparison to the findings of the present study, 10 factors were found to be modulated during infection, and only the upregulation of ApoE was confirmed. In contrast to the results obtained here, the other differentially expressed proteins were related to iron homeostasis, cell attachment, and metabolism. These differences may result from the different methods used to determine the cutoff value for significant fold changes (a minimum fold change of 1.5 [$P < 0.05$] in the present study compared to a minimum fold change of 0.1 [$P < 0.1$] in the previous study [26]). A previous study by Yu and collaborators analyzed the transcriptome of HEV genotype 1-infected chimpanzee liver (72). The two transcriptional factors Fos and HNF4A were found to be upregulated. In the present study, they were also identified when building the network describing the interaction of modulated factors. The other differences observed between the two analyses may be explained by the fact that a different genotype was used: genotype 1 infects only humans and is considered to be more virulent than genotype 3 (56). Also, the technical approaches in the two studies were different, and it is known that RNA levels may not always reflect protein levels.

To summarize, the present study reveals 61 proteins differentially expressed during hepatitis E virus infection. Analysis of these

proteins showed some differences between the three strains used in terms of cholesterol synthesis, lipid metabolism, and a possible inflammatory response of the host during infection. Moreover, some proteins involved in several viral life cycles—including HnRNPK, ApoE, PHB, and PP2A—were identified. Some of these proteins have previously been shown to interact with HEV ORF3 or ORF2. Altogether, the data obtained provide important guidance for further analysis of the pathogenesis of HEV and may help explain the various symptoms associated with this infection.

ACKNOWLEDGMENTS

S.R. and this work were supported by EC project PREDEMICS no. 278433.

We are grateful to Thomas Lilin and his collaborators, Francis Moreau, Mickael Jacob, and Mylène Bouillon from the Biomedical Research Center (CRBM) in Maisons-Alfort, France, for their care of the pigs and their contribution to the experiments performed with pigs. We thank Guilhem Clary from the Plateforme Electrophorese Bidimensionnelle, UMR 8104, for 2D-DIGE technical support. We also thank Cedric Broussard, Patrick Mayeux, and François Guillonneau from Proteomics Platform 3P5, Université Paris Descartes, for their technical support with MALDI-TOF/TOF MS. Our thanks go to Sylvain Bellier from the biochemistry laboratory of the National Veterinary School of Alfort for biochemical analyses. We also thank André Keranflech and Frédéric Paboeuf from ANSES Ploufragan for the SFP pig delivery in Maisons-Alfort, France.

REFERENCES

1. **Shams R, Khero RB, Ahmed T, Hafiz A.** 2001. Prevalence of hepatitis E virus (HEV) antibody in pregnant women of Karachi. J Ayub Med Coll Abbottabad **13:**31–35.
2. **Oncu S, Oncu S, Okyay P, Ertug S, Sakarya S.** 2006. Prevalence and risk factors for HEV infection in pregnant women. Med Sci Monit **12:**CR36–CR39.
3. **Kc S, Sharma D, Basnet BK, Mishra AK.** 2009. Effect of acute hepatitis E infection in patients with liver cirrhosis. J Nepal Med Assoc **48:**226–229.
4. **Lockwood GL, Fernandez-Barredo S, Bendall R, Banks M, Ijaz S, Dalton HR.** 2008. Hepatitis E autochthonous infection in chronic liver disease. Eur J Gastroenterol Hepatol **20:**800–803. http://dx.doi.org/10.1097/MEG.0b013e3282f1cbff.
5. **Kamar N, Izopet J.** 2014. Does chronic hepatitis E virus infection exist in immunocompetent patients? Hepatology **60:**427. http://dx.doi.org/10.1002/hep.26927.
6. **Emerson SU, Nguyen H, Graff J, Stephany DA, Brockington A, Purcell RH.** 2004. In vitro replication of hepatitis E virus (HEV) genomes and of an HEV replicon expressing green fluorescent protein. J Virol **78:**4838–4846. http://dx.doi.org/10.1128/JVI.78.9.4838-4846.2004.
7. **Ahmad I, Holla RP, Jameel S.** 2011. Molecular virology of hepatitis E virus. Virus Res **161:**47–58. http://dx.doi.org/10.1016/j.virusres.2011.02.011.
8. **Ansari IH, Nanda SK, Durgapal H, Agrawal S, Mohanty SK, Gupta D, Jameel S, Panda SK.** 2000. Cloning, sequencing, and expression of the hepatitis E virus (HEV) nonstructural open reading frame 1 (ORF1). J Med Virol **60:**275–283. http://dx.doi.org/10.1002/(SICI)1096-9071(200003)60:3<275::AID-JMV5>3.0.CO;2-9.
9. **Jameel S.** 1999. Molecular biology and pathogenesis of hepatitis E virus. Expert Rev Mol Med **1999:**1–16.
10. **Panda SK.** 2000. Hepatitis E virus: recent advances. Trop Gastroenterol **21:**47.
11. **Graff J, Torian U, Nguyen H, Emerson SU.** 2006. A bicistronic subgenomic mRNA encodes both the ORF2 and ORF3 proteins of hepatitis E virus. J Virol **80:**5919–5926. http://dx.doi.org/10.1128/JVI.00046-06.
12. **Emerson SU, Nguyen HT, Torian U, Burke D, Engle R, Purcell RH.** 2010. Release of genotype 1 hepatitis E virus from cultured hepatoma and polarized intestinal cells depends on open reading frame 3 protein and requires an intact PXXP motif. J Virol **84:**9059–9069. http://dx.doi.org/10.1128/JVI.00593-10.
13. **Smith DB, Simmonds P, members of the International Committee on the Taxonomy of Viruses Hepeviridae Study Group, Jameel S, Emerson SU, Harrison TJ, Meng X-J, Okamoto H, Van der Poel WHM, Purdy MA** 2014. Consensus proposals for classification of the family Hepeviridae. J Gen Virol **95**(Pt 10)**:**2223–2232. http://dx.doi.org/10.1099/vir.0.068429-0.
14. **Purcell RH, Emerson SU.** 2008. Hepatitis E: an emerging awareness of an old disease. J Hepatol **48:**494–503. http://dx.doi.org/10.1016/j.jhep.2007.12.008.
15. **Lu L, Li C, Hagedorn CH.** 2006. Phylogenetic analysis of global hepatitis E virus sequences: genetic diversity, subtypes and zoonosis. Rev Med Virol **16:**5–36. http://dx.doi.org/10.1002/rmv.482.
16. **Bouquet J, Tessé S, Lunazzi A, Eloit M, Rose N, Nicand E, Pavio N.** 2011. Close similarity between sequences of hepatitis E virus recovered from humans and swine, France, 2008-2009. Emerg Infect Dis **17:**2018–2025. http://dx.doi.org/10.3201/eid1711.110616.
17. **Oliveira-Filho EF, König M, Thiel H-J.** 2013. Genetic variability of HEV isolates: inconsistencies of current classification. Vet Microbiol **165:**148–154. http://dx.doi.org/10.1016/j.vetmic.2013.01.026.
18. **Schmidt T, Striebinger H, Haas J, Bailer SM.** 2010. The heterogeneous nuclear ribonucleoprotein K is important for herpes simplex virus-1 propagation. FEBS Lett **584:**4361–4365. http://dx.doi.org/10.1016/j.febslet.2010.09.038.
19. **Masuda J-I, Yano K, Tamada Y, Takii Y, Ito M, Omagari K, Kohno S.** 2005. Acute hepatitis E of a man who consumed wild boar meat prior to the onset of illness in Nagasaki, Japan. Hepatol Res **31:**178–183. http://dx.doi.org/10.1016/j.hepres.2005.01.008.
20. **Tei S, Kitajima N, Takahashi K, Mishiro S.** 2003. Zoonotic transmission of hepatitis E virus from deer to human beings. Lancet **362:**371–373. http://dx.doi.org/10.1016/S0140-6736(03)14025-1.
21. **Colson P, Borentain P, Queyriaux B, Kaba M, Moal V, Gallian P, Heyries L, Raoult D, Gerolami R.** 2010. Pig liver sausage as a source of hepatitis E virus transmission to humans. J Infect Dis **202:**825–834. http://dx.doi.org/10.1086/655898.
22. **Jiang X-S, Tang L-Y, Dai J, Zhou H, Li S-J, Xia Q-C, Wu J-R, Zeng R.** 2005. Quantitative analysis of severe acute respiratory syndrome (SARS)-associated coronavirus-infected cells using proteomic approaches: implications for cellular responses to virus infection. Mol Cell Proteomics **4:**902–913. http://dx.doi.org/10.1074/mcp.M400112-MCP200.
23. **Munday DC, Emmott E, Surtees R, Lardeau C-H, Wu W, Duprex WP, Dove BK, Barr JN, Hiscox JA.** 2010. Quantitative proteomic analysis of A549 cells infected with human respiratory syncytial virus. Mol Cell Proteomics **9:**2438–2459. http://dx.doi.org/10.1074/mcp.M110.001859.
24. **Coombs KM, Berard A, Xu W, Krokhin O, Meng X, Cortens JP, Kobasa D, Wilkins J, Brown EG.** 2010. Quantitative proteomic analyses of influenza virus-infected cultured human lung cells. J Virol **84:**10888–10906. http://dx.doi.org/10.1128/JVI.00431-10.
25. **Chan EY, Qian W-J, Diamond DL, Liu T, Gritsenko MA, Monroe ME, Camp DG, II, Smith RD, Katze MG.** 2007. Quantitative analysis of human immunodeficiency virus type 1-infected $CD4^+$ cell proteome: dysregulated cell cycle progression and nuclear transport coincide with robust virus production. J Virol **81:**7571–7583. http://dx.doi.org/10.1128/JVI.00288-07.
26. **Lee G, Han D, Song J-Y, Kim J-H, Yoon S.** 2011. Proteomic analysis of swine hepatitis E virus (sHEV)-infected livers reveals upregulation of apolipoprotein and downregulation of ferritin heavy chain. FEMS Immunol Med Microbiol **61:**359–363. http://dx.doi.org/10.1111/j.1574-695X.2010.00770.x.
27. **Thirant C, Galan-Moya E-M, Dubois LG, Pinte S, Chafey P, Broussard C, Varlet P, Devaux B, Soncin F, Gavard J, Junier M-P, Chneiweiss H.** 2012. Differential proteomic analysis of human glioblastoma and neural stem cells reveals HDGF as a novel angiogenic secreted factor. Stem Cells **30:**845–853. http://dx.doi.org/10.1002/stem.1062.
28. **Prévilon M, Le Gall M, Chafey P, Federeci C, Pezet M, Clary G, Broussard C, François G, Mercadier J-J, Rouet-Benzineb P.** 2013. Comparative differential proteomic profiles of nonfailing and failing hearts after in vivo thoracic aortic constriction in mice overexpressing FKBP12.6. Physiol Rep **1:**e00039. http://dx.doi.org/10.1002/phy2.39.
29. **Rose N, Lunazzi A, Dorenlor V, Merbah T, Eono F, Eloit M, Madec F, Pavio N.** 2011. High prevalence of hepatitis E virus in French domestic pigs. Comp Immunol Microbiol Infect Dis **34:**419–427. http://dx.doi.org/10.1016/j.cimid.2011.07.003.
30. **Bouquet J, Cheval J, Rogée S, Pavio N, Eloit M.** 2012. Identical consensus sequence and conserved genomic polymorphism of hepatitis E virus

during controlled interspecies transmission. J Virol **86:**6238–6245. http://dx.doi.org/10.1128/JVI.06843-11.
31. **Jothikumar N, Cromeans TL, Robertson BH, Meng XJ, Hill VR.** 2006. A broadly reactive one-step real-time RT-PCR assay for rapid and sensitive detection of hepatitis E virus. J Virol Methods **131:**65–71. http://dx.doi.org/10.1016/j.jviromet.2005.07.004.
32. **Barnaud E, Rogée S, Garry P, Rose N, Pavio N.** 2012. Thermal inactivation of infectious hepatitis E virus in experimentally contaminated food. Appl Environ Microbiol **78:**5153–5159. http://dx.doi.org/10.1128/AEM.00436-12.
33. **Livak KJ, Schmittgen TD.** 2001. Analysis of relative gene expression data using real-time quantitative PCR and the 2(−delta delta C(T)) method. Methods **25:**402–408. http://dx.doi.org/10.1006/meth.2001.1262.
34. **Hishiki T, Shimizu Y, Tobita R, Sugiyama K, Ogawa K, Funami K, Ohsaki Y, Fujimoto T, Takaku H, Wakita T, Baumert TF, Miyanari Y, Shimotohno K.** 2010. Infectivity of hepatitis C virus is influenced by association with apolipoprotein E isoforms. J Virol **84:**12048–12057. http://dx.doi.org/10.1128/JVI.01063-10.
35. **Tanaka T, Takahashi M, Kusano E, Okamoto H.** 2007. Development and evaluation of an efficient cell-culture system for hepatitis E virus. J Gen Virol **88**(Pt 3)**:**903–911. http://dx.doi.org/10.1099/vir.0.82535-0.
36. **Coller KE, Heaton NS, Berger KL, Cooper JD, Saunders JL, Randall G.** 2012. Molecular determinants and dynamics of hepatitis C virus secretion. PLoS Pathog **8:**e1002466. http://dx.doi.org/10.1371/journal.ppat.1002466.
37. **Mackenzie JM, Westaway EG.** 2001. Assembly and maturation of the flavivirus Kunjin virus appear to occur in the rough endoplasmic reticulum and along the secretory pathway, respectively. J Virol **75:**10787–10799. http://dx.doi.org/10.1128/JVI.75.22.10787-10799.2001.
38. **Blank CA, Anderson DA, Beard M, Lemon SM.** 2000. Infection of polarized cultures of human intestinal epithelial cells with hepatitis A virus: vectorial release of progeny virions through apical cellular membranes. J Virol **74:**6476–6484. http://dx.doi.org/10.1128/JVI.74.14.6476-6484.2000.
39. **Zhang H-L, Wu J, Zhu J.** 2010. The immune-modulatory role of apolipoprotein E with emphasis on multiple sclerosis and experimental autoimmune encephalomyelitis. Clin Dev Immunol **2010:**186813. http://dx.doi.org/10.1155/2010/186813.
40. **Hauser PS, Ryan RO.** 2013. Impact of apolipoprotein E on Alzheimer's disease. Curr Alzheimer Res **10:**809–817. http://dx.doi.org/10.2174/15672050113109990156.
41. **Zhang H, Wu J, Zhu J.** 2010. The role of apolipoprotein E in Guillain-Barré syndrome and experimental autoimmune neuritis. J Biomed Biotechnol **2010:**357412. http://dx.doi.org/10.1155/2010/357412.
42. **Kamar N, Bendall RP, Peron JM, Cintas P, Prudhomme L, Mansuy JM, Rostaing L, Keane F, Ijaz S, Izopet J, Dalton HR.** 2011. Hepatitis E virus and neurologic disorders. Emerg Infect Dis **17:**173–179. http://dx.doi.org/10.3201/eid1702.100856.
43. **Flower DR.** 1996. The lipocalin protein family: structure and function. Biochem J **318**(Pt 1)**:**1–14.
44. **Taneja S, Ahmad I, Sen S, Kumar S, Arora R, Gupta VK, Aggarwal R, Narayanasamy K, Reddy VS, Jameel S.** 2011. Plasma peptidome profiling of acute hepatitis E patients by MALDI-TOF/TOF. Proteome Sci **9:**5. http://dx.doi.org/10.1186/1477-5956-9-5.
45. **Taneja S, Sen S, Gupta VK, Aggarwal R, Jameel S.** 2009. Plasma and urine biomarkers in acute viral hepatitis E. Proteome Sci **7:**39. http://dx.doi.org/10.1186/1477-5956-7-39.
46. **Munshi SU, Taneja S, Bhavesh NS, Shastri J, Aggarwal R, Jameel S.** 2011. Metabonomic analysis of hepatitis E patients shows deregulated metabolic cycles and abnormalities in amino acid metabolism. J Viral Hepat **18:**e591–e602. http://dx.doi.org/10.1111/j.1365-2893.2011.01488.x.
47. **Kar-Roy A, Korkaya H, Oberoi R, Lal SK, Jameel S.** 2004. The hepatitis E virus open reading frame 3 protein activates ERK through binding and inhibition of the MAPK phosphatase. J Biol Chem **279:**28345–28357. http://dx.doi.org/10.1074/jbc.M400457200.
48. **Korkaya H, Jameel S, Gupta D, Tyagi S, Kumar R, Zafrullah M, Mazumdar M, Lal SK, Xiaofang L, Sehgal D, Das SR, Sahal D.** 2001. The ORF3 protein of hepatitis E virus binds to Src homology 3 domains and activates MAPK. J Biol Chem **276:**42389–42400. http://dx.doi.org/10.1074/jbc.M101546200.
49. **Surjit M, Varshney B, Lal SK.** 2012. The ORF2 glycoprotein of hepatitis E virus inhibits cellular NF-κB activity by blocking ubiquitination mediated proteasomal degradation of IκBα in human hepatoma cells. BMC Biochem **13:**7. http://dx.doi.org/10.1186/1471-2091-13-7.
50. **Watt AJ, Garrison WD, Duncan SA.** 2003. HNF4: a central regulator of hepatocyte differentiation and function. Hepatology **37:**1249–1253. http://dx.doi.org/10.1053/jhep.2003.50273.
51. **Chandra V, Kar-Roy A, Kumari S, Mayor S, Jameel S.** 2008. The hepatitis E virus ORF3 protein modulates epidermal growth factor receptor trafficking, STAT3 translocation, and the acute-phase response. J Virol **82:**7100–7110. http://dx.doi.org/10.1128/JVI.00403-08.
52. **Chandra V, Holla P, Ghosh D, Chakrabarti D, Padigaru M, Jameel S.** 2011. The hepatitis E virus ORF3 protein regulates the expression of liver-specific genes by modulating localization of hepatocyte nuclear factor 4. PLoS One **6:**e22412. http://dx.doi.org/10.1371/journal.pone.0022412.
53. **Bommer GT, MacDougald OA.** 2011. Regulation of lipid homeostasis by the bifunctional SREBF2-miR33a locus. Cell Metab **13:**241–247. http://dx.doi.org/10.1016/j.cmet.2011.02.004.
54. **Kim KH, Hong SP, Kim K, Park MJ, Kim KJ, Cheong J.** 2007. HCV core protein induces hepatic lipid accumulation by activating SREBP1 and PPARgamma. Biochem Biophys Res Commun **355:**883–888. http://dx.doi.org/10.1016/j.bbrc.2007.02.044.
55. **Kim KH, Shin H-J, Kim K, Choi HM, Rhee SH, Moon H-B, Kim HH, Yang US, Yu D-Y, Cheong J.** 2007. Hepatitis B virus X protein induces hepatic steatosis via transcriptional activation of SREBP1 and PPARgamma. Gastroenterology **132:**1955–1967. http://dx.doi.org/10.1053/j.gastro.2007.03.039.
56. **Halbur PG, Kasorndorkbua C, Gilbert C, Guenette D, Potters MB, Purcell RH, Emerson SU, Toth TE, Meng XJ.** 2001. Comparative pathogenesis of infection of pigs with hepatitis E viruses recovered from a pig and a human. J Clin Microbiol **39:**918–923. http://dx.doi.org/10.1128/JCM.39.3.918-923.2001.
57. **Lhomme S, Abravanel F, Dubois M, Sandres-Saune K, Rostaing L, Kamar N, Izopet J.** 2012. Hepatitis E virus quasispecies and the outcome of acute hepatitis E in solid-organ transplant patients. J Virol **86:**10006–10014. http://dx.doi.org/10.1128/JVI.01003-12.
58. **Bomsztyk K, Denisenko O, Ostrowski J.** 2004. hnRNP K: one protein multiple processes. Bioessays **26:**629–638. http://dx.doi.org/10.1002/bies.20048.
59. **Hsieh TY, Matsumoto M, Chou HC, Schneider R, Hwang SB, Lee AS, Lai MM.** 1998. Hepatitis C virus core protein interacts with heterogeneous nuclear ribonucleoprotein K. J Biol Chem **273:**17651–17659. http://dx.doi.org/10.1074/jbc.273.28.17651.
60. **Fan B, Lu K-Y, Reymond Sutandy FX, Chen Y-W, Konan K, Zhu H, Kao CC, Chen C-S.** 2014. A human proteome microarray identifies that the heterogeneous nuclear ribonucleoprotein K (hnRNP K) recognizes the 5′ terminal sequence of the hepatitis C virus RNA. Mol Cell Proteomics **13:**84–92. http://dx.doi.org/10.1074/mcp.M113.031682.
61. **Real CI, Megger DA, Sitek B, Jahn-Hofmann K, Ickenstein LM, John MJ, Walker A, Timm J, Kuhlmann K, Eisenacher M, Meyer HE, Gerken G, Broering R, Schlaak JF.** 2013. Identification of proteins that mediate the pro-viral functions of the interferon stimulated gene 15 in hepatitis C virus replication. Antiviral Res **100:**654–661. http://dx.doi.org/10.1016/j.antiviral.2013.10.009.
62. **Zhang W, Zhang X, Tian C, Wang T, Sarkis PTN, Fang Y, Zheng S, Yu X-F, Xu R.** 2008. Cytidine deaminase APOBEC3B interacts with heterogeneous nuclear ribonucleoprotein K and suppresses hepatitis B virus expression. Cell Microbiol **10:**112–121. http://dx.doi.org/10.1111/j.1462-5822.2007.01020.x.
63. **Lin J-Y, Li M-L, Huang P-N, Chien K-Y, Horng J-T, Shih S-R.** 2008. Heterogeneous nuclear ribonuclear protein K interacts with the enterovirus 71 5′ untranslated region and participates in virus replication. J Gen Virol **89**(Pt 10)**:**2540–2549. http://dx.doi.org/10.1099/vir.0.2008/003673-0.
64. **Tsai P-L, Chiou N-T, Kuss S, García-Sastre A, Lynch KW, Fontoura BMA.** 2013. Cellular RNA binding proteins NS1-BP and hnRNP K regulate influenza A virus RNA splicing. PLoS Pathog **9:**e1003460. http://dx.doi.org/10.1371/journal.ppat.1003460.
65. **Kuadkitkan A, Wikan N, Fongsaran C, Smith DR.** 2010. Identification and characterization of prohibitin as a receptor protein mediating DENV-2 entry into insect cells. Virology **406:**149–161. http://dx.doi.org/10.1016/j.virol.2010.07.015.
66. **Wintachai P, Wikan N, Kuadkitkan A, Jaimipuk T, Ubol S, Pulmanausahakul R, Auewarakul P, Kasinrerk W, Weng W-Y, Panyasrivanit**

M, Paemanee A, Kittisenachai S, Roytrakul S, Smith DR. 2012. Identification of prohibitin as a Chikungunya virus receptor protein. J Med Virol **84:**1757–1770. http://dx.doi.org/10.1002/jmv.23403.

67. **Dang S-S, Sun M-Z, Yang E, Xun M, Ma L, Jia Z-S, Wang W-J, Jia X-L.** 2011. Prohibitin is overexpressed in Huh-7-HCV and Huh-7.5-HCV cells harboring in vitro transcribed full-length hepatitis C virus RNA. Virol J **8:**424. http://dx.doi.org/10.1186/1743-422X-8-424.
68. **Liu C, Zhang A, Guo J, Yang J, Zhou H, Chen H, Jin M.** 2012. Identification of human host proteins contributing to H5N1 influenza virus propagation by membrane proteomics. J Proteome Res **11:**5396–5405. http://dx.doi.org/10.1021/pr3006342.
69. **Zhou T-B, Qin Y-H.** 2013. Signaling pathways of prohibitin and its role in diseases. J Recept Signal Transduct Res **33:**28–36. http://dx.doi.org/10.3109/10799893.2012.752006.
70. **Guergnon J, Godet AN, Galioot A, Falanga PB, Colle J-H, Cayla X, Garcia A.** 2011. PP2A targeting by viral proteins: a widespread biological strategy from DNA/RNA tumor viruses to HIV-1. Biochim Biophys Acta **1812:**1498–1507. http://dx.doi.org/10.1016/j.bbadis.2011.07.001.
71. **Duong FHT, Filipowicz M, Tripodi M, La Monica N, Heim MH.** 2004. Hepatitis C virus inhibits interferon signaling through up-regulation of protein phosphatase 2A. Gastroenterology **126:**263–277. http://dx.doi.org/10.1053/j.gastro.2003.10.076.
72. **Yu C, Boon D, McDonald SL, Myers TG, Tomioka K, Nguyen H, Engle RE, Govindarajan S, Emerson SU, Purcell RH.** 2010. Pathogenesis of hepatitis E virus and hepatitis C virus in chimpanzees: similarities and differences. J Virol **84:**11264–11278. http://dx.doi.org/10.1128/JVI.01205-10.